Physicochemical characteristics of rubberwood biomass and its thermal decomposition kinetics for thermochemical conversion applications

Pumin Kongto[1,2] · Arkom Palamanit[2] · Sumate Chaiprapat[3] · Nakorn Tippayawong[4] · Jarunee Khempila[5] · Jakkrawut Techo[6] · Makatar Wae-hayee[7]

Abstract

Thailand has plentiful rubberwood biomass for biofuel and bioenergy applications, as well as for carbon material production. One of the keys to choosing a biomass conversion process is its effects on the physicochemical properties. In addition, thermochemical conversion of biomass also requires knowledge of its thermal decomposition behavior and kinetics for reactor design; and specification of operating conditions. Thus, the aims of this research were to explore the physicochemical properties of rubberwood biomasses (RWBs) generated alternatively from branches, trunks, and roots. The rubberwood biomass with the best energy properties was then selected to investigate its thermal decomposition behavior and kinetics. The physicochemical properties of RWBs determined were the gross and elemental components, energy properties, lignocellulosic components, and major noncombustible elements. Thermal decomposition observations were carried out by using the thermogravimetric analyzer under a nitrogen atmosphere at heating rates of 5, 10, 20, and 30 °C min^{-1}. The kinetic analysis was conducted by applying the iso-conversional model-free methods of Friedman, Kissinger–Akahira–Sunose (KAS), and Ozawa–Flynn–Wall (OFW). Based on statistical analysis, the results highlighted that the trunks (RTT) possessed the best energy properties. The lignocellulosic and elemental components of RWBs had small differences. The activation energy derived from iso-conversional methods demonstrated consistency with previous studies. The activation energies were in the ranges 159.11–210.61, 168.89–175.06, and 169.96–176.01 kJ mol^{-1} according to the Friedman, KAS, and OFW methods, respectively. These explorations are useful for applying the RWB as feedstock in torrefaction and pyrolysis applications.

Keywords Biomass thermal decomposition · Biomass decomposition kinetics · Physicochemical properties of biomass · Rubberwood biomass · Kinetic parameters

✉ Arkom Palamanit
arkom.p@psu.ac.th

1 Energy Technology Program, Department of Interdisciplinary Engineering, Faculty of Engineering, Prince of Songkla University, 15 Kanjanavanich Rd., Hat Yai 90110, Songkhla, Thailand

2 Biomass Energy and Sustainable Technologies (BEST) Research Center, Energy Technology Program, Department of Interdisciplinary Engineering, Faculty of Engineering, Prince of Songkla University, 15 Kanjanavanich Rd., Hat Yai 90110, Songkhla, Thailand

3 Department of Civil and Environmental Engineering, Faculty of Engineering, Prince of Songkla University, 15 Kanjanavanich Rd., Hat Yai 90110, Songkhla, Thailand

4 Department of Mechanical Engineering, Chiang Mai University, 239 Huay Kaew Rd., Muang District, Chiang Mai 50200, Thailand

5 Physics Program, Faculty of Science and Technology, Rajabhat Maha Sarakham University, 80 Nakhon Sawan Rd., Mueang District, Maha Sarakham 44000, Thailand

6 Division of Industrial Technology, Faculty of Agricultural Technology and Industrial Technology, Nakhon Sawan Rajabhat University, Nakhon Sawan, Thailand

7 Department of Mechanical and Mechatronics Engineering, Faculty of Engineering, Prince of Songkla University, Hat Yai 90110, Songkhla, Thailand

Introduction

Rubberwood biomass, among the biomass resources available in Thailand, is particularly abundant on the southern peninsula. In 2022, Thailand had around 3.85 million hectares of rubber plantations [1]. When old rubber trees, typically aged between 25 and 30 years, are replanted, a substantial volume of rubberwood biomass is generated. It has been suggested that replanting these trees results in approximately 13 tons per hectare of branches, 74 tons per hectare of roots, and 250 tons per hectare of trunks. In addition, various types of biomass are generated during the processing of rubber tree trunks into lumber or timber, including bark, slabs, and sawdust [2]. In Thailand, biomass obtained from rubberwood is widely used to generate heat and power, as well as biomass pellets. This biomass is of particular interest due to its various advantages, such as avoiding direct conflict with food crops, having a large annual generation, and a low cost. Large pieces of rubberwood biomass are usually chopped into rubberwood chips. Which are then used as solid fuels in industrial settings, where they are utilized to generate heat, steam, and electricity in biomass-fired power plants. The industrial consumption of this biomass to produce heat is normally by combustion or firing. Currently, there is interest in and challenges associated with converting rubberwood biomass through thermochemical processes, for instance gasification, torrefaction, or pyrolysis. These processes are significant for transforming biomass into high-grade biofuels or products [3]. In these three thermochemical processes, thermal decomposition behavior of a biomass during heating involves complex processes, both physical and chemical. Thus, on using rubberwood biomass via torrefaction, pyrolysis, or gasification, an understanding of its physicochemical properties by different sections of the tree is important.

The design of biomass processing, operational conditions, and desired products are all heavily influenced by the physicochemical characteristics of lignocellulosic biomass. By the way of nature, each biomass has different physical and chemical characteristics dependent on species, variety, geographic locality, weather, and age. In thermochemical processing, these aspects strongly influence product yield and characteristics, and production costs. An example of this is when biomass, characterized by high moisture levels and low lignin content, undergoes torrefaction, resulting in reduced product yield and increased energy costs [4]. Furthermore, the torrefaction of biomass that contains significant amounts of chlorine (Cl), potassium (K), sodium (Na), and silicon (Si) results in torrefied biomass with higher concentrations of these elements. This, consequently, causes problems in further

combustion or firing processes [5]. This is because of a tendency for slagging and fouling. Besides torrefaction, pyrolysis is also popular for biochar and bio-oil production. Slow pyrolysis is normally applied for biochar production. Typically, slow pyrolysis, a thermal conversion technique, is utilized to produce biochar. The biochar products and characteristics are significantly influenced by the particle size, proportions of lignocellulosic components, and elemental contents. The biomass particles' size, moisture and oxygen content, and proportions of lignocellulosic components all influence the yield and quality of bio-oil produced by fast pyrolysis. In a higher temperature process like gasification, the biomass is decomposed to synthesis gas used for heating, power, or valuable chemical products. The physical features and chemical components of biomass affect both synthesis gas yield and composition (in non-condensable gaseous components and tar content). Moreover, they also affect the reactions in each zone of a gasifier, as well as having side effects in ash formation and its fusion. Previous research by Chen et al. [6] has shown that lignocellulosic biomass containing significant amounts of hemicellulose tends to yield comparatively high amounts of liquid or gaseous products during thermal decomposition. On the other hand, pyrolysis or torrefaction applied to biomass rich in cellulose and lignin yields a higher percentage of solid product. This is mostly because the behavior of biomass thermal degradation varies depending on temperature and lignocellulosic component content. According to Yang et al. [7], during pyrolysis, hemicellulose and cellulose decompose at temperatures ranging from 220 to 315 °C and 315 to 400 °C, respectively, while lignin breaks down over the wide 160–900 °C temperature range.

Kinetic analysis is frequently used to determine how biomass will decompose thermally. Such investigation is important for designing the reactor, for feasibility assessment, and for scaling in industrial applications [8]. There are two types of approaches to evaluating solid-state kinetic data. These include model-fitting methods and model-free methods. By fitting multiple models to the provided dataset, model-fitting algorithms enable the determination of the apparent activation energy (E_a) and the pre-exponential factor (A). Model-free procedures, on the other hand, do not make any assumptions about a specific model; rather, instead they estimate the activation energy by using either the conversion factor or the temperature. They are typically more complicated, necessitating additional understanding to fully comprehend the reaction mechanisms. Several publications have thoroughly examined Friedman, KAS, and OFW, three well-known model-free approaches for computing kinetic parameters. Thermogravimetric analysis is a common method for studying the kinetics of pyrolysis. It determines the mass

loss in a sample as a function of temperature (or time). Numerous studies have delved into comprehending the pyrolysis behavior and kinetics across various types of biomass, including wood sawdust [9], sugarcane bagasse [10], banana leaves [11], residual rubber seed cake and shell [12], rice husk and elephant grass [13], rice and corn [14], and wheat straw and groundnut stalk [15]. However, only few studies have concentrated on rubberwood biomass. This study concentrated on investigating the thermal decomposition kinetics and physicochemical properties of rubberwood biomass. Additionally, knowing the activation energy is important for reactor design, feasibility evaluation, and scaling. TGA was used to execute pyrolysis, and thermal response curves at various linear heating rates were acquired. To determine the activation energy and pre-exponential factor, three model-free non-isothermal techniques were utilized. Additionally, a study investigated the impact of heating rate on the thermal decomposition of rubberwood biomass.

Materials and methods

Rubberwood biomass preparation

In the first section of the study, rubberwood biomass from different parts of rubber trees was prepared and characterized to compare the compositions. The variety of rubber trees was RRIM 600, and they were 28 years old. The Khlong Thom district in Krabi province, which is situated in Thailand, was the location where these rubber trees were cultivated. The whole rubber tree, including its roots, was cut down and separated into three parts, namely rubber tree branches (RTB) (without the leaves), rubber tree trunks (RTT), and rubber tree roots (RTR). Then, each type of fresh biomass was reduced in size by sawing and chopping to rubberwood chips with sizes below 40 mm. This step was performed by a large-scale chopping machine at a rubberwood factory in Songkhla province, Thailand. The wood chips underwent further size reduction using a machine for chopping (MCH-420, Machinery789, Thailand) to attain particle sizes less than 5 mm. Subsequently, solar energy was employed to dry this biomass until its moisture content dropped below 10% (on a wet basis). After drying, the sample was ground into flour using a grinding machine (Bonny, 2HP, Thailand) fitted with a 2 mm sieve. The resulting RWB was stored in tightly sealed plastic bags for future analysis. All biomass samples had their fuel properties determined and reported. The type of rubberwood biomass with the best energy properties was then selected for use as feedstock in determinations of thermal decomposition behavior and kinetics.

Characteristics of rubberwood biomass

Physicochemical characteristics and energy properties

Following proximate analysis, the following components of RWB were identified: moisture content (MC), volatile matter (VM), ash content (AC), and fixed carbon content (FC). The method described in ASTM D7582-15 was followed using a macro thermogravimetric analyzer (TGA 701, LECO, USA) [16]. The experiment was conducted three times. The data are presented as mean percentages by mass (% on a received basis) together with their corresponding standard deviations. The percentages of elemental carbon (C), hydrogen (H), nitrogen (N), and sulphur (S) in the RWB were determined using a CHNS/O analyzer (FLASH 2000, ThermoScientific, Italy) during the ultimate analysis. Additionally, an internal procedure was employed for this determination [17]. Differencing ($C + H + N + O + S + AC + MC = 100\%$) was used to calculate the oxygen (O) content [18]. The results are presented as means of percentages by mass (% on a received basis) with standard deviations. The calculations were performed three times. The neutral detergent fiber (NDF), acid detergent fiber (ADF), and acid detergent lignin (ADL) were used to determine the proportions of hemicellulose (HCL), cellulose (CL), lignin (LN), and other (extractives and ash) in RWB, as outlined in previous research [19] (Eqs. 1–4). The calculations were repeated three times, and the averages of the percentages by mass with standard deviations (% on a dry basis) are reported as the results.

$$\text{Cellulose content } (CL) = ADF - ADL \tag{1}$$

$$\text{Hemicellulose content } (HCL) = NDF - ADF \tag{2}$$

$$\text{Lignin content } (LN) = ADL \tag{3}$$

$$\text{Other } = 100 - CL - HCL - LN \tag{4}$$

where CL, HCL, and LN represent the percentages of cellulose, hemicellulose, and lignin in RWB on a dry basis.

RWB energy contents are expressed as lower heating value (LHV) and higher heating value (HHV). The correlations shown in Eqs. (5–6) were utilized for estimation purposes. The computations were dependent on the results of the ultimate analyses [20]. It is well-known that these correlations exhibit low root mean square error (RMSE) and high coefficient of determination (R^2). The findings, generated in triplicate, are presented as means with standard deviations in MJ kg^{-1}.

$$LHV = -5.5232 + 0.2373N + 0.4334C \\ + 0.2360H + 0.3732S + 0.000838O \tag{5}$$

$$HHV = -4.9140 + 0.2611N + 0.4114C \\ + 0.6114H + 0.3888S + 0.02097O \tag{6}$$

where C, H, N, O and S denote the percentages of carbon, hydrogen, nitrogen, oxygen, and sulphur in RWB on a dry basis.

The bulk density of RWB was computed by dividing the mass of the sample (in kg) by the volume (in m^3) of a container with known dimensions (modified from Zhang et al. [21]). Subsequently, the energy density (ED) (in MJ m^{-3}) of RWB was determined using Eq. (7), employing the bulk density (in kg m^{-3}) and the higher heating value (in MJ kg^{-1}), in accordance with earlier research [22].

$$ED = HHV \times Bulk\ density \tag{7}$$

where *HHV* represents the RWB's higher heating value on an as-received basis (MJ kg^{-1}).

Using Inductively Coupled Plasma Optical Emission Spectrometry (ICP-OES, AVIO500, Perkin Elmer Instruments, USA), the primary mineral components in RWB samples were identified. The findings included the reported quantities of calcium (Ca), cadmium (Cd), iron (Fe), potassium (K), magnesium (Mg), sodium (Na), lead (Pb), and silicon (Si). The results are presented as means (mg kg^{-1}) with standard deviations. The calculations were performed three times.

Statistical analysis

The PSPP program was used to conduct the statistical analyses, including an analysis of variance (ANOVA). The purpose of this task was to identify significant variations in the data. If the data exhibited a normal distribution ($p > 0.05$), the Tukey test was employed. In contrast, data that did not follow a normal distribution ($p \leq 0.05$) were subjected to the Games-Howell test.

### Thermal decomposition behavior and kinetics

RWB samples underwent thermogravimetric analyses using a thermogravimetric analyzer (TGA7, Perkin Elmer Ltd., USA). Method WI-RES-TGA-001 and an internal thermogravimetric technique based on ASTM E1131 were employed to measure mass loss. Ten mg of a precisely weighed biomass sample were placed in an aluminum crucible for TGA analysis. A homogeneously distributed powdered biomass sample was heated at rates of 5, 10, 20, and 30 °C min^{-1} to record its thermal degradation profile under a nitrogen atmosphere, with the temperature ranging from 50 to 1000 °C. For each biomass sample, the mass loss and mass loss percentage were recorded along with the temperature change (% °C^{-1}). Using Origin Pro software and TGA data, the DTG curves of biomass samples were generated. The results show the derivative of mass loss (% min^{-1}). In this study, it was considered for 150–900 °C temperatures. The mass loss below 150 °C was attributed to the loss of volatiles and moisture [23], while the mass loss above 900 °C was negligible. As a result, the "onset" and "completion" temperatures of biomass thermal degradation were defined as 150 °C and 900 °C, respectively. Consequently, model-free techniques were employed in the kinetic analysis, which was based on TGA data within this temperature range.

Kinetics approach conceptually

Thermal decomposition of biomass during the torrefaction process involves complex chemical reactions. Kinetic analysis is a popular method to identify the characteristics of biomass thermal degradation. This kinetic investigation is important for designing the reactor, for feasibility assessment, and for scaling in industrial applications [8]. Both isothermal and non-isothermal runs are basic modes of biomass pyrolysis. There are several alternative models, like the one-step model (called model-free) [24], the two-step model [25], the multi-step model [26], and the multi-component model [27, 28]. Through an examination of the non-isothermal solid-state kinetics, it is possible to get the activation energy (E_a) and the pre-exponential coefficient (A) as kinetic parameters. These parameters are derived from the results of the TGA. These data are of major interest in the context of combustion. Model-free methods are used to estimate $f(\alpha)$ of Eq. (9) at progressive conversion degrees in the absence of a reaction model [29].

The one-step global model operates on the assumption that the devolatilization of raw materials into final products is a single-step process. In this model, volatiles are defined as the total of gas and tar [30].

$$Biomass \xrightarrow{k} Volatiles + Char \tag{8}$$
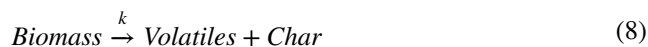
The general Eq. (9) provides the rate of conversion of solid biomass into volatile products through heat degradation.

$$\frac{d\alpha}{dt} = k(T)f(\alpha) \tag{9}$$

where in that order α, t, k(T), and $f(\alpha)$ represent the extent of conversion, time, rate constant, and reaction model, respectively.

The uniform kinetic reaction of the samples allows us to write $f(\alpha)$ as

$$f(\alpha) = (1 - \alpha)^n \tag{10}$$

where n is the order of reaction, with the case $n = 1$ called first order, and α is the extent of conversion. During the thermal decomposition, the extent (or degree) of conversion (α) is defined as follows:

$$\alpha = \frac{m_0 - m_t}{m_0 - m_f} \tag{11}$$

where m_0, m_t and m_f are the initial mass of the sample (mg), the mass of the sample at the moment (mg), and final mass of the sample (mg), respectively. Temperature affects the kinetic rate constant (k), typically provided by the Arrhenius equation as

$$k(T) = A \exp\left(-\frac{E_a}{RT}\right) \tag{12}$$

where A, E_a, R, *and* T denote the pre-exponential factor (s^{-1}), the activation energy of the decomposition reaction (kJ mol^{-1}), the universal gas constant (8.314 J mol^{-1} K^{-1}), and the absolute temperature (K).

Following the substitution of Eqs. (10) and (12) into Eq. (9), the following kinetic equation for biomass decomposition is obtained:

$$\frac{d\alpha}{dt} = A \exp\left(-\frac{E_a}{RT}\right)(1 - \alpha)^n \tag{13}$$

In non-isothermal thermogravimetric experiments, the heating rate (β) is varied between runs, while held constant in each run, and then the temperature of pyrolysis is [31]

$$T = T_0 + \beta t \tag{14}$$

where T, T_0, t and β are the temperature, initial temperature, time, and heating rate.

$$dT = d(T_0 + \beta t) = \beta dt \tag{15}$$

$$dt = \frac{dT}{\beta} \tag{16}$$

Thus, Eq. (13) becomes,

$$\frac{d\alpha}{dT} = \frac{A}{\beta} \exp\left(-\frac{E_a}{RT}\right)(1 - \alpha)^n \tag{17}$$

Rearranging Eq. (17) and integrating from T_0 to T for temperature and from 0 to α for extent gives Eq. (18):

$$G(\alpha) = \int_0^\alpha \frac{d\alpha}{f(\alpha)} = \int_{T_0}^T \frac{A}{\beta} \exp\left(-\frac{E_a}{RT}\right) dT \tag{18}$$

where G(α) is the integrated form of the conversion dependence function $f(\alpha)$. There is no explicit formula in terms of elementary functions for Eq. (18). Therefore, to address this complicated integral, Eq. (18) can only be solved using either numerical integration or approximations.

Model-free methods

It is not necessary to assume any reaction model to use model-free approaches. The Kinetics Committee of the International Confederation for Thermal Analysis and Calorimetry (ICTAC) recommends utilizing curves with varying heating rates for an equivalent degree of conversion to calculate kinetic parameters [29]. Model-free methods have two main advantages: they are simple to use and eliminate errors associated with selecting a kinetic model. Kissinger–Akahira–Sunose (KAS), Kissinger, Ozawa–Flynn–Wall (OFW), Friedman, and Vyazovkin (V) are the most well-known practitioners of iso-conversional methods [32, 33]. In this study, model-free techniques from Friedman, OFW, and KAS have been applied [30, 34].

Friedman method

Because this model contains a derivative in its defining equation, this method differs from the other model-free methods adopted here. The Friedman method is the first model-free method that is iso-conversional. Equation (17) can be re-arranged as follows [32],

$$\beta \cdot \frac{d\alpha}{dT} = A \, \exp \cdot \left(-\frac{E_a}{RT}\right) f(\alpha) \tag{19}$$

Once the natural logarithms of both sides of Eq. (19) have been determined,

$$\ln\left(\beta \frac{d\alpha}{dT}\right) = \ln\left[Af(\alpha)\right] - \left(\frac{E_a}{RT}\right) \tag{20}$$

The activation energy (E_a) can be determined from the slope of the plot of $\ln\left(\beta \frac{d\alpha}{dT}\right)$ against $\frac{-1}{T}$ (K) at a constant conversion extent.

Ozawa–Flynn–Wall (OFW)

The integral iso-conversion methods are based on varying assumptions regarding the integral terms in Eq. (9). Instead of using the temperature integral, the OFW approach utilized the linear Doyle approximation, i.e., $p(x) = \exp(-5.331 - 1.052x)$,

where $x = -\frac{E_a}{RT}$. Therefore, the mathematical expression obtained is that shown in Eq. (21) [33, 35].

$$\ln \beta = \ln \left[\frac{AE_a}{RG(\alpha)} \right] - 5.331 - 1.052 \left(\frac{E_a}{RT} \right) \quad (21)$$

At each degree of conversion, the three pairs of $\ln \beta$ and $1/T$ data points obtained for three heating rates are plotted and fit with a straight line. Then, the activation energy, E_a, is calculated from the slope that equals $(-1.052 \frac{E_a}{RT})$ [30, 36].

Kissinger–Akahira–Sunose method (KAS)

Biomass pyrolysis kinetics studies frequently use the KAS method, as indicated by its widespread presence in academic literature [37]. KAS method used the simple approximation for exponential integral, i.e., $p(x) = x^{-2}e^{-x}$ [33], the final equation is as follows [38]:

$$\ln \left(\frac{\beta}{T^2} \right) = \ln \left[\frac{AR}{E_a G(\alpha)} \right] - \frac{E_a}{RT} \quad (22)$$

At each degree of conversion, the three pairs of $\ln \left(\frac{\beta}{T^2} \right)$ and $\frac{1}{T}$ data points obtained on using three heating rates are plotted and fit with a straight line. The slope, $\left(\frac{E_a}{R} \right)$, is used to compute the activation energy, E_a [32].

Results and discussion

Properties of rubberwood biomass

Table 1 summarizes the features of rubberwood biomasses from various parts of the tree, namely RTB, RTT, and RTR. The study investigated various properties, such as lignocellulosic compositions, gross components, major elements, heating values, bulk densities, and energy densities. Statistically significant differences ($p \leq 0.05$) were observed between the rubberwood biomass sections. In RTB, RTT, and RTR, the contents of CL, HCL, LN, and other materials were found to be, respectively, 59.29–64.46%, 12.52–13.66%, 16.71–17.04%, and 5.96–10.01%. The contents of CL, HCL, LN, and other in RWB showed significant differences ($p \leq 0.05$). RTB had a higher CL compared to

Table 1 Properties of rubberwood biomass by section of rubber tree

Component of different sections			
Properties	RTB	RTT	RTR
Lignocellulosic compositions (%, dry basis)			
Cellulose	$64.46^a \pm 0.18$	$63.69^b \pm 0.33$	$59.29^c \pm 0.22$
Hemicellulose	$12.56^b \pm 0.18$	$12.52^b \pm 0.14$	$13.66^a \pm 0.48$
Lignin	$17.02^a \pm 0.09$	$16.71^b \pm 0.12$	$17.04^a \pm 0.12$
Other[d]	$5.96^c \pm 0.14$	$7.08^b \pm 0.16$	$10.01^a \pm 0.19$
Proximate analysis (%, as received basis)			
Moisture content	$5.39^a \pm 0.05$	$4.60^c \pm 0.03$	$5.02^b \pm 0.06$
Fixed carbon	$16.09^a \pm 0.21$	$15.84^a \pm 0.17$	$15.26^b \pm 0.14$
Volatile matter	$77.06^a \pm 0.16$	$77.78^a \pm 0.17$	$77.30^a \pm 0.12$
Ash content	$1.47^b \pm 0.08$	$1.53^b \pm 0.01$	$2.42^a \pm 0.01$
Ultimate analysis (%, as received basis)			
Carbon	$44.86^b \pm 0.11$	$45.15^a \pm 0.03$	$44.83^b \pm 0.17$
Hydrogen	$5.82^b \pm 0.14$	$6.04^a \pm 0.05$	$6.00^a \pm 0.04$
Nitrogen	$0.18^b \pm 0.00$	$0.17^b \pm 0.00$	$0.24^a \pm 0.00$
Oxygen[e]	$42.26^a \pm 0.14$	$42.50^a \pm 0.02$	$41.49^b \pm 0.26$
Sulphur	$0.02^a \pm 0.00$	$0.00^a \pm 0.00$	$0.00^a \pm 0.00$
Heating value (MJ kg^{-1}, dry basis)			
Lower heating value	$16.57^a \pm 0.03$	$16.56^a \pm 0.01$	$16.52^a \pm 0.08$
Higher heating value	$19.35^a \pm 0.06$	$19.41^a \pm 0.02$	$19.35^a \pm 0.09$
Bulk density (kg m^{-3})	$220.10^b \pm 5.83$	$253.18^a \pm 2.20$	$188.30^c \pm 2.20$
Energy density (MJ m^{-3})	$3.97^b \pm 0.12$	$4.63^a \pm 0.04$	$3.41^c \pm 0.04$
Major metallic elements (mg kg^{-1})			
Calcium	3185 ± 48.47	3376 ± 35.37	3599 ± 10.78
Cadmium	< 0.403	< 0.403	< 0.403
Iron	94.62 ± 0.292	118.6 ± 1.02	214.6 ± 2.23
Potassium	6531 ± 102.50	5791 ± 65.88	5087 ± 87.94
Magnesium	511.0 ± 1.45	667.1 ± 4.27	1222 ± 9.09
Sodium	17.15 ± 0.844	12.94 ± 0.495	20.78 ± 1.859
Lead	< 1.715	< 1.715	< 1.715
Silicon	85.18 ± 7.864	73.06 ± 6.036	179.8 ± 1.33

Different lowercase letters (a, b, or c) in the same row indicate statistically significant differences by ANOVA ($p \leq 0.05$)

[d]Calculated by difference (CL + HCL + LN + Other = 100%)

[e]Calculated by difference (C + H + N + O + S + AC + MC = 100%)

both RTT and RTR, while RTR exhibited higher HCL, LN, and other components than RTB. Biomass type and lignocellulosic composition are critical factors to consider during torrefaction. This is because a biomass with high CL and LN tends to yield more solid products [6, 39]. Additionally, a high lignin content in biomass can naturally act as an adhesive in torrefied biomass pellets [40]. Conversely, when biomass with high HCL is subjected to torrefaction at a high temperature, it tends to produce more liquid product than solids by mass yield [41]. The lignocellulosic composition of RWB shows a lower HCL content compared to LN and

CL, which is similar to woody biomasses like pine wood and spruce wood [42]. Moreover, RWB exhibits higher CL and LN contents in its lignocellulosic composition compared to non-woody biomasses such as sugarcane leaves [43], oil palm fronds, and oil palm trunks, despite having a lower HCL content [17].

Fresh RTB, RTT, and RTR initially had moisture contents of 43.60, 41.52, and 39.38%, respectively. The final moisture contents of RTB, RTT, and RTR decreased to 5.39, 4.60, and 5.02%, respectively, after the completion of the preparation and sun drying processes. The gross components (FC, VM, and AC) of RWB (rubberwood biomass) ranged within 15.26–16.09, 77.06–77.78, and 1.47–2.42%, respectively. RTB had a higher FC than RTT and RTR, but the difference from RTT was not statistically significant ($p > 0.05$). In contrast, the VM content was higher in RTB than in RTT and RTR. Moreover, the AC content of RTR was higher than those of RTB and RTT. RWB has proportions of FC, VM, and AC similar to other woody biomasses, including logging residue chips [44], pine, and eucalyptus [45]. In comparison to both wood-based and non-wood-based biomasses, such as banana, leucaena, sugarcane bagasse, sugarcane leaves, bamboo, and rice straw, RWB exhibits a higher VM content. On the other hand, RWB has a lower VM than certain biomasses, such as beech, leucaena, pine wood chip, and willow. RWB has a higher FC content compared to woody biomasses like pine wood chips, sawdust, and beech. However, RWB has a lower ash content compared to non-woody biomasses, such as sugarcane leaves, bamboo, cotton stalk, and rice straw [43, 46]. The amount of moisture in biomass plays a critical role in its efficiency as a solid fuel for combustion. Biomass with a high MC necessitates more energy to evaporate the water during combustion or co-firing, leading to thermal energy losses in the process [47]. Moreover, a high MC in biomass can result in biological decomposition during storage and transportation, as well as moisture absorption in high humidity conditions [4]. Conversely, biomass with a lower moisture content can have a longer shelf life with minimal risk of biological degradation. Furthermore, it becomes less expensive to transport solid biomass that is resistant to water absorption because less moisture needs to be transported with the biomass [48]. Fixed carbon refers to the carbon that remains in the char after devolatilization in pyrolysis, excluding ash and moisture [45, 49]. In the biomass thermochemical conversion, fixed carbon is a crucial parameter that influences solids yield. More fixed carbon leads to a higher yield of solids. Additionally, a higher fixed carbon content also translates into longer burning times as well as decreased smoke production. Conversely, volatile matter, which can be classified as condensable or non-condensable, refers to the vapor released during fuel heating. It comprises volatile organic and inorganic gases containing nitrogen and sulphur, as well as carbon (iv) oxide [45].

The volatile components of biomass typically consist of a blend of aromatic and short-chain hydrocarbons. A higher content of volatiles indicates easier ignition and subsequent gasification or oxidation of the biomass [48]. In solid fuel combustion, the ignition temperature is a significant factor influenced directly by both MC and VM quantities. Fuels with lower MC and higher VM content typically ignite more readily [50]. Moreover, a high FC and a low VM increase the fuel ratio (FC/VM), resulting in less smoke and emissions during combustion or co-firing [51]. In this approach, more effective usage of biomass is encouraged via the process of co-firing with coal [52]. However, the fuel ratio of biomass fuel should not exceed 2 for it to be suitable for co-firing with coal [53]. Conversely, a low fuel ratio leads to difficulties in controlling burnout, increased flaming combustion, reduced char combustion, incomplete fuel combustion, and more smoke emissions [54]. Ash in biomass refers to the non-volatile and non-combustible component [55]. The species and locality of the biomass plantation area significantly influence the chemical composition of ash. Ashes from agricultural biomass, containing varying amounts of phosphorus, potassium, sodium, and chlorine, are influenced by factors such as available nutrients, soil quality, fertilizers, and weather patterns [56]. Understanding the ash content is crucial in selecting the most suitable combustion and ash cleaning technologies [57]. However, ash is not ideal for solid fuel applications as it can cause several issues related to its management and disposal, including slag formation and fouling in the boiler. However, the ash content of RWB is relatively low compared to many other biomasses, such as citrus tree wood, beech wood sawdust, eucalyptus bark, oak branches, palm kernel shells, and corn crop [58]. When it comes to combustion or co-firing, the ash content plays a major role in the design of the combustion chamber, the exhaust cleaning system (which includes a cyclone, bag filter, and ESP), and the ash removal system. Biomass that contains a high percentage of ash has the potential to result in the generation of slag and fouling as a result of the melting of ash at high combustion temperatures. These issues can increase maintenance costs and downtime of the power plant [59].

The organic elements of RTB, RTT, and RTR are very similar. The carbon, hydrogen, nitrogen, oxygen, and sulphur contents were in the ranges 44.83–45.15, 5.82–6.04, 0.17–0.24, 41.49–42.50, and 0–0.02%, respectively. RTT exhibited a higher carbon content compared to RTB and RTR. However, RTT did not ($p > 0.05$) differ significantly from RTB and RTT in this regard. The oxygen contents of RTR and RTT did not ($p > 0.05$) differ significantly from RTB, but they had higher oxygen contents. The organic elements of RWB were found to be nearly identical to those of beach wood and willow [45]. During combustion, C and H undergo exothermic reactions, forming carbon dioxide (CO_2)

and water (H_2O). The presence of both C and H enhances the higher heating value. Nevertheless, hydrogen contributes to the lower heating value through water formation. While the oxygen content has a negative effect, biomass with high oxygen content is considered a low-grade fuel because of its lower heating value [45]. Although the complete combustion of biomass releases CO_2, plants utilize CO_2 during the growth stage. Hence, CO_2 has not been added to the atmosphere as a result. This is referred to as zero carbon emissions or the carbon cycle [60]. However, in the case of incomplete combustion, there is an increase in the release of carbon-based pollutants, such as carbon monoxide, hydrocarbons, and other harmful substances, into the atmosphere [61]. During combustion, nitrogen is almost entirely converted to gaseous N_2 and some nitric oxides (NO_x [NO, NO_2]). Modern solid biofuel furnaces have extremely low release levels of nitrous oxide (N_2O). The ash contains only a trace amount of N. The main variables influencing NO_x formation include air supply, furnace type, combustion temperature, and the type of combustion technology used [62]. In the meantime, the sulphur (S) present in solid biofuel predominantly becomes gaseous SO_2; and alkali as well as earth-alkali sulphates. During the process of the flue gas cooling in the boiler section, sulfur dioxide (SO_x) either combines directly with fine fly ash particles that are deposited on heat exchanger surfaces or produces sulfates and condenses on the surfaces of the heat exchanger. For optimal performance, biomass should contain a high proportion of organic matter with low ash content, moisture content, oxygen, and suphur contents, along with high density and favorable grinding properties [63]. The heating value of rubberwood biomass consists of both LHV and HHV. The lower heating values of RTB, RTT, and RTR were in the range 16.52–16.57 MJ kg^{-1}, while their higher heating values were in the range 19.35–19.41 MJ kg^{-1}. Both the LHV and HHV of RWB did not ($p > 0.05$) differ significantly. The HHV of RWB was higher than that of wood biomass, such as cedarwood [64] and patula pine, according to previous studies [65]. However, the HHV of RWB was close to those of bark, stem wood, and stumps of Norway spruce [66]. Compared to most fossil fuels, biomass typically has a lower heating value, particularly when expressed in terms of volume. This is attributed to its low mass density and high oxygen content [61].

Furthermore, the bulk densities of RTB, RTT, and RTR were in the range 188.30–253.18 kg m^{-3}. There was a significant difference in the bulk density as RTT had a higher bulk density than RTB, and RTR was significantly different ($p \leq 0.05$) from both RTT and RTB, resulting in RTT having a higher energy density than RTB and RTR. The energy density of RTT was 4.63 GJ m^{-3}, whereas the energy densities of RTB and RTR were 3.97 and 3.41 GJ m^{-3}, respectively. The bulk density of biomass feedstock significantly affects its energy density, along with storage, transportation, and handling costs [67]. Higher bulk densities reduce transportation and storage costs by greater masses to be moved or stored in fixed-volume containers [57]. Moreover, the major metallic elements calcium, cadmium, iron, potassium, magnesium, sodium, lead, and silicon, are shown in the bottom part of Table 1. The results show that the rubberwood biomasses have high potassium and calcium contents. The potassium of RTB, RTT, and RTR was in the range 5087–6531 mg kg^{-1}, whereas Ca was in the range 3185–3599 mg kg^{-1}. These elements are essential contributors to ash melting, deposit formation, fly ash and aerosol emissions, corrosion (in conjunction with S and Cl), and ash utilization/disposal. The melting behavior of ash is affected by both its major and minor elements. Ca and Mg tend to make the melting point of ash higher, while K tends to make it lower [68].

Although the initial parameters of the rubberwood biomass results (RTB, RTT, and RTR) are almost identical, statistically significant differences ($p \leq 0.05$) were observed. The results revealed a significant difference in cellulose contents between roots, trunks, and branches of rubberwood. Additionally, the ash content of RTR is significantly higher than those of RTB and RTT by about 58–65%. Generally, high cellulose and lignin contents lead to a higher solid yield. Therefore, the properties of RTB seem more suitable than those of RTR and RTT. However, when considering the heating value and bulk density of RTT, it is higher than those of RTB and RTR, which results in the energy density of RTT being greater. RTT had the highest content of volatile matter, making it easy to ignite, and the lowest content of moisture. Therefore, based on the above results, RTT was chosen in this study for use as the material on determining the thermal decomposition behavior and kinetics.

Thermal decomposition behavior at different heating rates

The TGA and DTG profiles of rubberwood biomass subjected to heating rates of 5, 10, 20, and 30 min^{-1} in a nitrogen environment are presented in Fig. 1a and b. Thermogravimetric analysis and differential thermogravimetric investigations provide insights and data regarding biomass behavior during thermal degradation. They are frequently utilized to study thermal conversion characteristics. For a typical biomass containing cellulose, hemicellulose, and lignin, TGA and DTG studies are employed to ascertain the overall sequence of degradation reactions and the kinetic properties of the entire pyrolysis process. It is seen that there are four stages of mass loss of RWB during heating in an inert atmosphere over 50–1000 °C, including dehydration, stationary stage, devolatilization, and char formation [69]. The RWB has a fractional change in mass

Fig. 2 Iso-conversional lines of RWB were generated using the Friedman method at different conversion rates
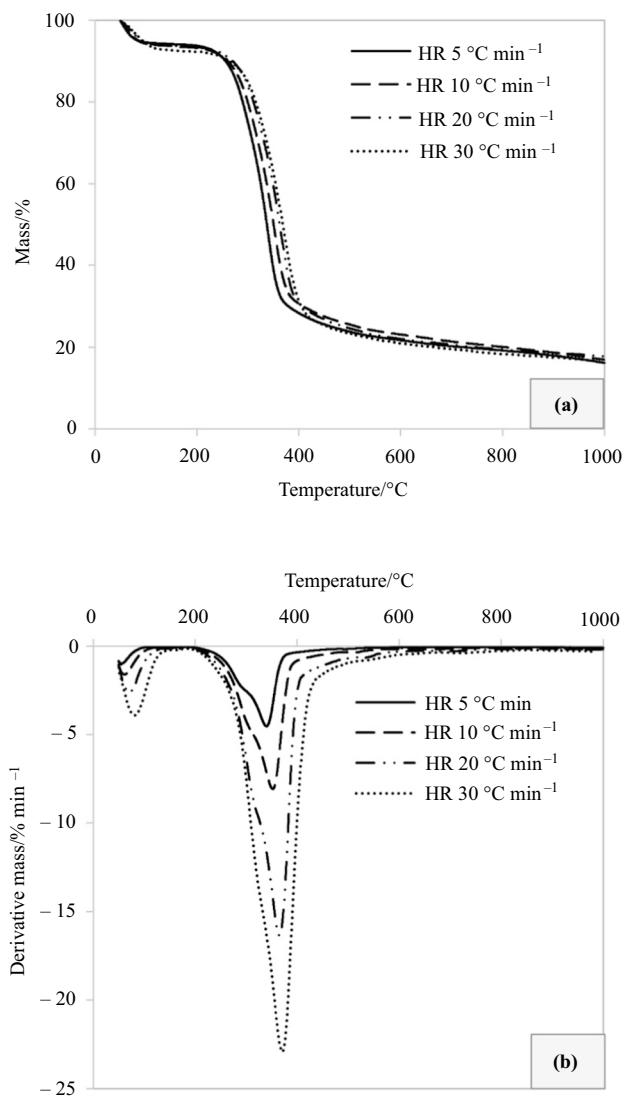
Fig. 1 Thermal decomposition profiles of rubberwood biomass (RTT) at different heating rates in a nitrogen gas atmosphere: (a) TGA, and (b) DTG curves

during each stage. The first stage occurred at 50–105 °C, where moisture evaporation (the drying stage) caused a slight decrease in mass. The remaining mass percentage (%) of the RWB has decreased to 95.03% during torrefaction at 105 °C. As a result of the sample's earlier pretreatment, a considerably lower amount of moisture is evaporated from the torrefied sample. The drying step (T < 105 °C) is not considered in the pyrolysis analysis, as the focus of this research lies on the thermal decomposition process. The mass of biomass was relatively constant in the next stage (110–200 °C), which can be observed from the DTG line. This occurs because the majority of the moisture has already evaporated, and the supplied heat is primarily utilized to elevate the sample temperature. This phase is commonly referred to as the "heating up stage".
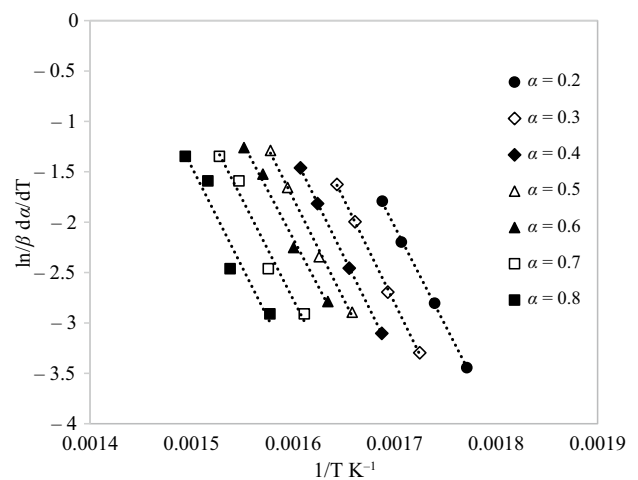
Then, between temperatures of 200 and 450 °C, devolatilization occurred. At higher temperatures, a larger quantity of volatile matter was lost from the raw sample, with the remaining mass decreasing from 93.99 to 26.56% of the initial mass; in contrast, the torrefied sample under the same temperature conditions released a smaller amount of volatile matter. The primary cause of the significant alteration is the thermal breakdown of lignocellulosic materials, specifically hemicellulose and cellulose. The final step, which resulted in the formation of char, occurred at temperatures exceeding 450 °C, attributed primarily to lignin decomposition.

Non-isothermal TGA and DTG results for RWB samples at different heating rates are illustrated in Fig. 1a and b. Given the consistent trends observed in the TGA curves across these different heating rates, it is reasonable to conclude that varying the heating rate has a minimal impact on the overall reaction mechanism [70]. Thermal decomposition shifted to a higher temperature zone as the heating rate was increased, without harming decomposition. The fact that biomass is a poor conductor of heat might be one reason for the change in the TGA curve. This could namely result in a thermal lag (temperature gradient) in the cross-section of biomass [71]. When the heating rate was raised, the response peak shifted to a higher temperature and gained amplitude, as shown by the thermogravimetric analysis and derivative thermogravimetric curves of the RWB samples at each of the four different heating rates. These changes in behavior are due to a shift in the response mechanism as well as a poor transfer of heat. Lower heating rates are advantageous since they enable a gradual heating process for biomass particles, promoting improved heat transfer to the biomass interior. A higher heating rate releases a larger number of volatile
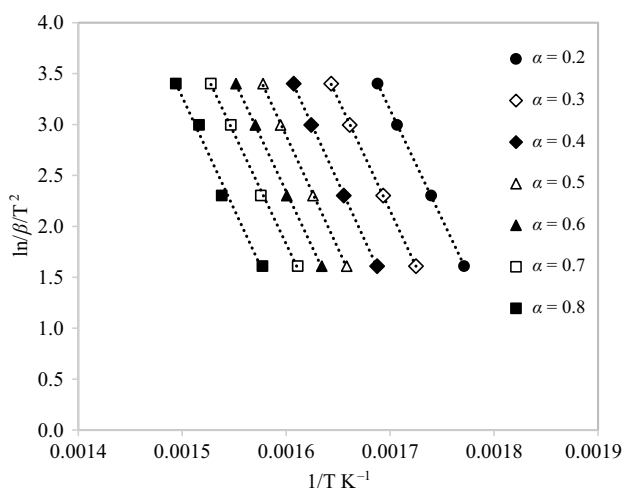
Fig. 3 Iso-conversional lines of RWB were generated using the OFW method at different conversion rates
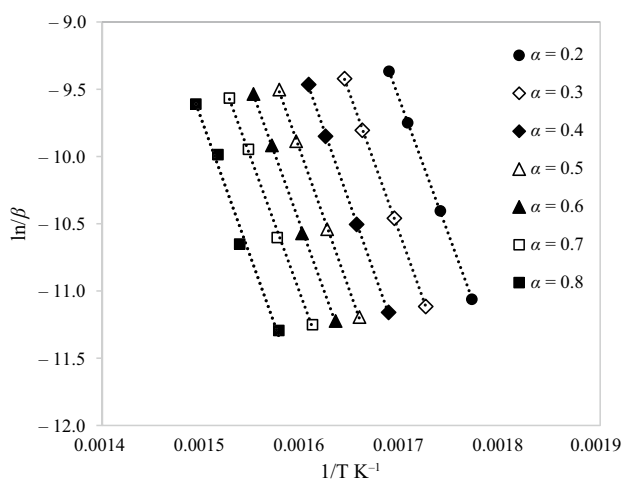

Fig. 4 Iso-conversional lines of RWB were generated using the KAS method at different conversion rates

components and lowers the residue remaining after torrefaction [30].

Thermal decomposition kinetics

The decomposition kinetics during RWB torrefaction were determined by using the three iso-conversional methods. Model-free methods were used to determine the activation energy (E_a) and pre-exponential factor (A) of RWB across a range of conversion rates ($0.2 \leq \alpha \leq 0.8$). Figures 2–4 depict the iso-conversional lines generated using the three methods (Friedman method, OFW method, and KAS method). The slopes and intercepts of linear plots generated using

the different model-free iso-conversional methods were used to calculate activation energies and pre-exponential factors shown in Table 2.

Table 2 displays the kinetic parameters. A conversion range of 0.2–0.8 was selected since the correlation factor was found to be relatively low when the conversion was larger than 0.8. The R^2 of all curves in the example plots for the torrefaction process were within the tight interval 0.9354–0.9999, showing excellent precision of the results and indicating that the points were well fit. Table 2 shows the values of E_a calculated by the Friedman, OFW, and KAS methods, which were in the ranges 159.11–210.61, 169.96–176.01, and 168.89–175.06 kJ mol^{-1}, respectively. The average values given by these methods were 172.31, 173.11, and 171.87 kJ mol^{-1}. The estimates of E_a demonstrate that the Friedman, OFW, and KAS methods provide very similar activation energies. Moreover, an observed tendency in these results matches the findings of other studies [33, 34]: according to the results, the E_a estimated using the KAS method was slightly lower compared to that obtained from the OFW method, whereas the Friedman method showed higher sensitivity to conversion rate variations. The different approximations used to calculate the temperature integral caused differences across methods [33]. The activation energy is determined by the pyrolysis reaction mechanism and is the minimal energy required to initiate a reaction. Higher activation energy indicates a lower reaction rate [71]. During the early stages of pyrolysis, there was an escalation in the apparent activation energy. It indicates endothermic activity, whereas a decrease in activation energy indicates exothermic activity [30]. At high conversion extents ($\alpha \geq 0.6$), the biomass samples have lost the majority of their low molecular weight components (holocellulose) and volatiles, leaving only thermally resistant high molecular weight (polyaromatic) lignin components and char with some ash. This showed mostly an increase in activation energy [23]. The pre-exponential factor (A) estimated by Friedman, OFW, and KAS methods was in the range 5.079×10^{12}–2.021×10^{16}, 8.170×10^{16}–5.158×10^{17}, and 5.520×10^{10}–4.084×10^{11} s^{-1}, respectively. The pre-exponential factor was less than 10^9 s^{-1}. The system is less reactive and is rate limited by the surface reaction. If the reactions are not surface area dependent, a low A value may suggest a closed complex [72]. Values higher than 10^9 s^{-1} suggest a highly reactive system and the formation of a simple complex. A value of A higher than 10^{14} s^{-1} indicates a slower and more difficult degrading effect and a higher rate of molecular collisions is required. In this instance, more reaction energy is required [32, 73]. The fluctuation in A with conversion is due to the sample's complex composition, and complicated reactions occur throughout the

Table 2 The kinetic parameters of rubberwood biomass were calculated using the Friedman, OFW, and KAS methods

Degree of conversion	Friedman method		
α	E_a/kJ mol^{-1}	A/s^{-1}	R^2
0.2	163.33	5.171×10^{13}	0.9994
0.3	171.20	1.380×10^{14}	0.9992
0.4	170.07	7.289×10^{13}	0.9999
0.5	167.08	3.158×10^{13}	0.9958
0.6	159.11	5.709×10^{12}	0.9912
0.7	164.72	1.225×10^{13}	0.9676
0.8	210.61	2.021×10^{16}	0.9354
Avg	172.31	2.931×10^{15}	0.9841
Degree of conversion	OFW method		
α	E_a/kJ mol^{-1}	A/s^{-1}	R^2
0.2	169.69	3.718×10^{17}	0.9999
0.3	173.03	4.440×10^{17}	0.9999
0.4	176.01	5.158×10^{17}	0.9996
0.5	175.43	3.240×10^{17}	0.9995
0.6	172.29	1.335×10^{17}	0.9994
0.7	171.02	8.170×10^{16}	0.9981
0.8	174.32	9.745×10^{16}	0.9864
Avg	173.11	2.812×10^{17}	0.9975
Degree of conversion	KAS method		
α	E_a/kJ mol^{-1}	A/s^{-1}	R^2
	KAS method		
0.2	168.89	3.019×10^{11}	0.9999
0.3	172.15	3.552×10^{11}	0.9999
0.4	175.06	4.084×10^{11}	0.9996
0.5	174.28	2.456×10^{11}	0.9995
0.6	170.81	9.446×10^{10}	0.9994
0.7	169.32	5.520×10^{10}	0.9979
0.8	172.56	6.553×10^{10}	0.9847
Avg	171.87	2.180×10^{10}	0.9973

decomposition [72]. The lower values at high conversion rates indicate lower reactivity of the process at the near completion of the reaction [73].

The activation energy variations as a function of conversion degree are shown in Fig. 5. The minimal energy needed to initiate a reaction is known as activation energy. A reaction requiring a high activation energy is hard to initiate. Activation energy is also used to determine the reactivity of a fuel. According to Fig. 5, three zones can be observed. E_a increased in the first zone ($\alpha = 0.2$–0.4) before progressively decreasing in the second zone ($\alpha = 0.4$–0.6). When the conversion was more than 0.4, it continued to decline, and then rapidly increased. HCL, CL, and LN are arranged based on their activation energy, ranging from low to high. The activation energy of RWB did not increase much in the first zone. This is because RWB has less than 13% hemicellulose.

When the conversion extent was 0.7, the activation energy increased, due to lignin's greater activation energy in the last zone of the process. Furthermore, the E_a of RWB had a similar trend to that of pinewood. He et al. discovered that the pyrolysis activation energy of pinewood remained largely constant [33].

Table 3 presents a comparison of calculated kinetic parameters, including instances from other studies. The activation energy estimates were obtained from iso-conversional models (Friedman, KAS, and OFW) in this study. The key findings were remarkably similar to those reported for other types of biomass. It is important to consider that reaction kinetics are influenced by temperature, and that the degradation temperature varies by biomass composition, which, in turn, depends on the soil conditions in which it is grown. Consequently, slight variations in the activation energy of
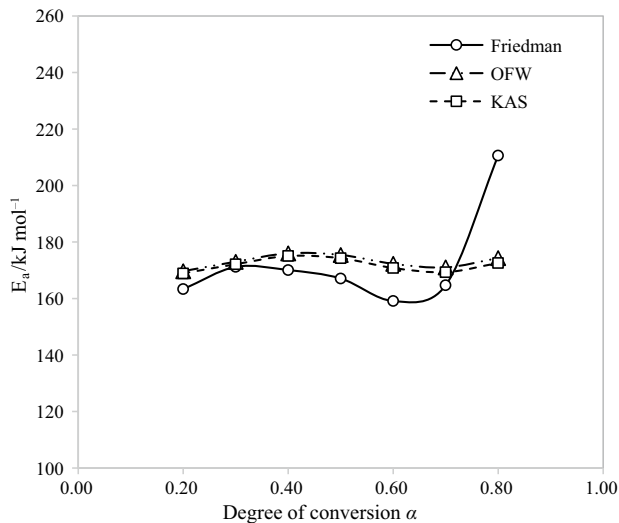
Fig. 5 Iso-conversional estimates of activation energy versus conversion

biomass could be attributed to these factors. Additionally, it is worth noting that the activation energy estimate is influenced by the mathematical calculations and the experimental conditions of a study.

Thermochemical conversion applications

Thermochemical processes are methods that utilize thermal energy or heat to modify the chemical composition of biomass to generate desired products. These processes can operate under inert or oxidative conditions, depending on the selected process. Currently, using such methods is widely accepted when converting biomass into energy sources (like power or heat) or various forms of fuels (including solids, liquids, and gasses). Operating parameters such as

reaction duration and temperature, oxygen supply, and reactor type, all influence the type of fuel or energy generated through the process. The classification of thermochemical processes is based on the temperature range and the reaction type. A low temperature (200–300 °C) and no air or oxygen are required for torrefaction to produce torrefied biomass, a solid fuel that resembles coal. At higher temperatures, the process becomes pyrolysis, which operates at temperatures of 400–800 °C without air or oxygen. This process is used to produce either biochar or bio-oil, depending on the type of pyrolysis, which can be slow or fast. In the case of biochar production, slow pyrolysis is appropriate. Gasification is a partial oxidation process, operated at a temperature of 700–1300 °C. The primary product of this process is synthesis gas, commonly known as syngas, which serves as a gaseous fuel for generating both electricity and heat. The last process is combustion, targeting complete oxidation at a temperature ranging within 700–1500 °C. During combustion, sufficient/excess air or oxygen needs to be supplied into the combustion chamber. The main desired product from combustion is heat for generating hot air, hot gas, steam, or hot oil [78]. Determining the appropriate product type also depends on the physicochemical characteristics of the biomass feedstock.

Torrefaction conditions, as well as the chemical and physical properties of the initial biomass, influence the yield and characteristics of the final thermochemical product. Biomass feedstock with high hemicellulose content tends to produce more liquid or gas products, while feedstock with high cellulose and lignin contents leads to higher solid product yields. The thermal decomposition rates vary depending on the proportions of lignocellulosic materials and temperature. The thermal decomposition of biomass during thermochemical processing involves complex chemical reactions [7]. Kinetic analysis is a popular method used to understand the

Table 3 Comparison of mean activation energy estimates of biomasses by iso-conversional methods

Type of biomass	Heating rate °C min^{-1}	Average value of activation energy /kJ mol^{-1}			References
		Friedman method	KAS method	OFW method	
Rubberwood biomass	5, 10, 20, and 30	172.31	171.78	173.11	This study
Pine sawdust	5, 10, 15, 20, and 25	168.58	171.66	179.29	[71]
Castor residue	5, 10, 15, 20, 30, and 40	–	165.85	–	[30]
Sugarcane leaves	5, 10, 15, 20, 30, and 40	239.58	226.75	–	[70]
Acacia	10, 20, and 30	–	–	190.45	[35]
Pine	10, 20, and 30	–	–	191.14	
Miscanthus	10, 20, and 30	–	–	207.93	
Prosopis juliflora wood	2, 5, 10, 15, 20, and 25	219.3	204	203.2	[34]
Rice husk	10, 20, and 30	–	72.3	–	[74]
Cherry seed	5–40	274.6	–	–	[75]
Karanj fruit hulls	5, 10, and 20	–	61.06	–	[76]
Maize cob	5, 10, and 20	197.63	185.39	–	[77]

characteristics of a biomass as regards its thermal degradation. This kinetic investigation is essential for designing the reactor, assessing its feasibility, and scaling it for industrial applications [8].

Conclusions

The main aim of this study was to explore the physicochemical properties of rubberwood biomasses (RWBs) obtained from different sections of the tree, specifically branches, trunks, and roots. The rubberwood biomass section with the best energy properties was then selected to investigate its thermal decomposition behavior and kinetics. The physicochemical properties of RWBs determined were gross and elemental compositions, energy properties, lignocellulosic component proportions, and major noncombustible elements. The thermal decomposition behavior of RWBs was investigated using a thermogravimetric analyzer (TGA) in a nitrogen environment at heating rates of 5, 10, 20, and 30 °C min^{-1}. The activation energy and decomposition kinetics were calculated using iso-conversional model-free methods, including Friedman, KAS, and OFW. Based on the obtained results, it can be concluded that all the RWBs had rather similar physicochemical properties. However, the biomass from the trunk section had the best energy properties as indicated by statistical analysis. The combustible components, lignocellulosic compositions and earth elements of RWBs were slightly different. In an inert atmosphere, the volatile components of RWBs were mainly released in the temperature range 340–372 °C. The thermal decomposition rate increased with higher heating rates. The activation energy estimates for thermal decomposition of rubberwood trunk, from the methods of KAS, OFW, and Friedman, were 168.89–175.06, 169.96–176.01, and 159.11–210.61 kJ mol^{-1}, respectively.

Author contributions Pumin Kongto: conceptualization, methodology, resources, data curation, writing—Original draft. Arkom Palamanit: conceptualization, writing—reviewing and editing, supervision, funding acquisition. Sumate Chaiprapat: conceptualization, reviewing and editing. Nakorn Tippayawong: conceptualization, reviewing and editing. Jarunee Khempila: writing—original draft preparation, reviewing and editing. Jakkrawut Techo: reviewing and editing. Makatar Waehayee: reviewing and editing.

Declarations

References

1. Office of Agricultural Economics. Agricultural Economic Information. 2022. https://www.oae.go.th/view/1/Home/EN-US. Accessed 3 Nov 2022
2. Office of Industrial Economics (OIE). Industrial cooperation development, final report, neighbouring countries project (industrial cooperation development strategy under the Indonesia-Malaysia-Thailand Growth Triangle: IMT-GT). 2013.
3. Verma M, Godbout S, Brar SK, Solomatnikova O, Lemay SP, Larouche JP. Biofuels production from biomass by thermochemical conversion technologies. Int J Chem Eng. 2012;2012:542426. https://doi.org/10.1155/2012/542426.
4. Medic D, Darr M, Shah A, Potter B, Zimmerman J. Effects of torrefaction process parameters on biomass feedstock upgrading. Fuel. 2012;91(1):147–54. https://doi.org/10.1016/j.fuel.2011.07.019.
5. Zhu Y, Niu Y, Tan H, Wang X. Short review on the origin and countermeasure of biomass slagging in grate furnace. Front Energy Res. 2014;2:7. https://doi.org/10.3389/fenrg.2014.00007.
6. Chen D, Gao A, Cen K, Zhang J, Cao X, Ma Z. Investigation of biomass torrefaction based on three major components: hemicellulose, cellulose, and lignin. Energy Convers Manag. 2018;169:228–37. https://doi.org/10.1016/j.enconman.2018.05.063.
7. Yang H, Yan R, Chen H, Lee DH, Zheng C. Characteristics of hemicellulose, cellulose and lignin pyrolysis. Fuel. 2007;86(12):1781–8. https://doi.org/10.1016/j.fuel.2006.12.013.
8. Dhyani V, Bhaskar T. A comprehensive review on the pyrolysis of lignocellulosic biomass. Renew Energy. 2018;129:695–716. https://doi.org/10.1016/j.renene.2017.04.035.
9. Varma AK, Mondal P. Physicochemical characterization and pyrolysis kinetics of wood sawdust. Energy Source Part Recov Util Environ Eff. 2016;38(17):2536–44. https://doi.org/10.1080/15567036.2015.1072604.
10. Silva JE, Calixto GQ, de Almeida CC, Melo DMA, Melo MAF, Freitas JCO, et al. Energy potential and thermogravimetric study of pyrolysis kinetics of biomass wastes. J Therm Anal Calorim. 2019;137(5):1635–43. https://doi.org/10.1007/s10973-019-08048-4.
11. Singh RK, Pandey D, Patil T, Sawarkar AN. Pyrolysis of banana leaves biomass: physico-chemical characterization, thermal decomposition behavior, kinetic and thermodynamic analyses. Bioresour Technol. 2020;310:123464. https://doi.org/10.1016/j.biortech.2020.123464.
12. Reshad AS, Tiwari P, Goud VV. Thermal decomposition and kinetics of residual rubber seed cake and shell. J Therm Anal Calorim. 2017;129(1):577–92. https://doi.org/10.1007/s10973-017-6136-4.
13. Braga RM, Melo DMA, Aquino FM, Freitas JCO, Melo MAF, Barros JMF, et al. Characterization and comparative study of pyrolysis kinetics of the rice husk and the elephant grass. J Therm

Anal Calorim. 2014;115(2):1915–20. https://doi.org/10.1007/s10973-013-3503-7.

14. Yao C, Wang X, Zhou Y, Jin X, Song L, Hu Y, et al. Thermogravimetric analysis and kinetics characteristics of typical grains. J Therm Anal Calorim. 2021;143(1):647–59. https://doi.org/10.1007/s10973-019-09213-5.

15. Gajera B, Tyagi U, Sarma AK, Jha MK. Impact of torrefaction on thermal behavior of wheat straw and groundnut stalk biomass: kinetic and thermodynamic study. Fuel Commun. 2022;12:100073. https://doi.org/10.1016/j.jfueco.2022.100073.

16. Palamanit A, Khongphakdi P, Tirawanichakul Y, Phusunti N. Investigation of yields and qualities of pyrolysis products obtained from oil palm biomass using an agitated bed pyrolysis reactor. Biofuel Res J. 2019;6(4):1065–79. https://doi.org/10.18331/BRJ2019.6.4.3.

17. Shrivastava P, Khongphakdi P, Palamanit A, Kumar A, Tekasakul P. Investigation of physicochemical properties of oil palm biomass for evaluating potential of biofuels production via pyrolysis processes. Biomass Convers Biorefinery. 2020. https://doi.org/10.1007/s13399-019-00596-x.

18. Basu P. Biomass gasification and pyrolysis: practical design and theory. Chichester: Elsevier; 2010.

19. Kongto P, Palamanit A, Chaiprapat S, Tippayawong N, Khempila J, Lam SS, et al. Physicochemical changes and energy properties of torrefied rubberwood biomass produced by different scale moving bed reactors. Renew Energy. 2023;219:119542. https://doi.org/10.1016/j.renene.2023.119542.

20. Ozyuguran A, Akturk A, Yaman S. Optimal use of condensed parameters of ultimate analysis to predict the calorific value of biomass. Fuel. 2018;214:640–6. https://doi.org/10.1016/j.fuel.2017.10.082.

21. Zhang Y, Ghaly A, Li B-X. Availability and physical properties of residues from major agricultural crops for energy conversion through thermochemical processes. Am J Agric Biol Sci. 2012;7:312–21. https://doi.org/10.3844/ajabssp.2012.312.321.

22. Kumar Singh R, Sarkar A, Chakraborty JP. Effect of torrefaction on the physicochemical properties of pigeon pea stalk (*Cajanus cajan*) and estimation of kinetic parameters. Renew Energy. 2019;138:805–19.

23. Muigai HH, Choudhury BJ, Kalita P, Moholkar VS. Co–pyrolysis of biomass blends: characterization, kinetic and thermodynamic analysis. Biomass Bioenergy. 2020;143:105839. https://doi.org/10.1016/j.biombioe.2020.105839.

24. Chen D, Zhou J, Zhang Q. Effects of heating rate on slow pyrolysis behavior, kinetic parameters and products properties of moso bamboo. Bioresour Technol. 2014;169:313–9. https://doi.org/10.1016/j.biortech.2014.07.009.

25. Bui H-H, Tran K-Q, Chen W-H. Pyrolysis of microalgae residues—a kinetic study. Bioresour Technol. 2016;199:362–6. https://doi.org/10.1016/j.biortech.2015.08.069.

26. Cavagnol S, Sanz E, Nastoll W, Roesler JF, Zymla V, Perré P. Inverse analysis of wood pyrolysis with long residence times in the temperature range 210–290 °C: selection of multi-step kinetic models based on mass loss residues. Thermochim Acta. 2013;574:1–9. https://doi.org/10.1016/j.tca.2013.09.009.

27. Bach Q-V, Chen W-H. A comprehensive study on pyrolysis kinetics of microalgal biomass. Energy Convers Manag. 2017;131:109–16. https://doi.org/10.1016/j.enconman.2016.10.077.

28. Wang S, Dai G, Yang H, Luo Z. Lignocellulosic biomass pyrolysis mechanism: a state-of-the-art review. Prog Energy Combust Sci. 2017;62:33–86. https://doi.org/10.1016/j.pecs.2017.05.004.

29. Vyazovkin S, Burnham AK, Criado JM, Pérez-Maqueda LA, Popescu C, Sbirrazzuoli N. ICTAC Kinetics Committee recommendations for performing kinetic computations on thermal analysis data. Thermochim Acta. 2011;520(1):1–19. https://doi.org/10.1016/j.tca.2011.03.034.

30. Kaur R, Gera P, Jha MK, Bhaskar T. Pyrolysis kinetics and thermodynamic parameters of castor (*Ricinus communis*) residue using thermogravimetric analysis. Bioresour Technol. 2018;250:422–8. https://doi.org/10.1016/j.biortech.2017.11.077.

31. Sajjad Ahmad M, Liu H, Alhumade H, Hussain Tahir M, Çakman G, Yıldız A, et al. A modified DAEM: to study the bioenergy potential of invasive Staghorn Sumac through pyrolysis, ANN, TGA, kinetic modeling, FTIR and GC–MS analysis. Energy Convers Manag. 2020;221:113173. https://doi.org/10.1016/j.enconman.2020.113173.

32. Yuan X, He T, Cao H, Yuan Q. Cattle manure pyrolysis process: Kinetic and thermodynamic analysis with isoconversional methods. Renew Energy. 2017;107:489–96. https://doi.org/10.1016/j.renene.2017.02.026.

33. He Q, Ding L, Gong Y, Li W, Wei J, Yu G. Effect of torrefaction on pinewood pyrolysis kinetics and thermal behavior using thermogravimetric analysis. Bioresour Technol. 2019;280:104–11. https://doi.org/10.1016/j.biortech.2019.01.138.

34. Chandrasekaran A, Ramachandran S, Subbiah S. Determination of kinetic parameters in the pyrolysis operation and thermal behavior of *Prosopis juliflora* using thermogravimetric analysis. Bioresour Technol. 2017;233:413–22. https://doi.org/10.1016/j.biortech.2017.02.119.

35. Wilk M, Magdziarz A, Gajek M, Zajemska M, Jayaraman K, Gokalp I. Combustion and kinetic parameters estimation of torrefied pine, acacia and *Miscanthus giganteus* using experimental and modelling techniques. Bioresour Technol. 2017;243:304–14. https://doi.org/10.1016/j.biortech.2017.06.116.

36. Sharara M, Sadaka S. Thermogravimetric analysis of Swine manure solids obtained from farrowing, and growing-finishing farms. J Sustain Bioenergy Syst. 2014;04:75–86. https://doi.org/10.4236/jsbs.2014.41008.

37. Doyle CD. Estimating isothermal life from thermogravimetric data. J Appl Polym Sci. 1962;6(24):639–42. https://doi.org/10.1002/app.1962.070062406.

38. Ozawa T. Estimation of activation energy by isoconversion methods. Thermochim Acta. 1992;203:159–65. https://doi.org/10.1016/0040-6031(92)85192-X.

39. Selvasembian R, Balasubramanian B. The potential of lignocellulosic biomass precursors for biochar production: performance, mechanism and wastewater application—a review. Ind Crops Prod. 2019;128:405–23. https://doi.org/10.1016/j.indcrop.2018.11.041.

40. Pelaez-Samaniego MR, Yadama V, Garcia-Perez M, Lowell E, McDonald AG. Effect of temperature during wood torrefaction on the formation of lignin liquid intermediates. J Anal Appl Pyrolysis. 2014;109:222–33. https://doi.org/10.1016/j.jaap.2014.06.008.

41. Zhao C, Shao Q, Ma Z, Li B, Zhao X. Physical and chemical characterizations of corn stalk resulting from hydrogen peroxide presoaking prior to ammonia fiber expansion pretreatment. Ind Crops Prod. 2016;83:86–93. https://doi.org/10.1016/j.indcrop.2015.12.018.

42. Negi S, Jaswal G, Dass K, Mazumder K, Elumalai S, Roy JK. Torrefaction: a sustainable method for transforming of agri-wastes to high energy density solids (biocoal). Rev Environ Sci Biotechnol. 2020;19(2):463–88. https://doi.org/10.1007/s11157-020-09532-2.

43. Khempila J, Kongto P, Meena P. Comparative study of solid biofuels derived from sugarcane leaves with two different thermochemical conversion methods: wet and dry torrefaction. BioEnergy Res. 2021. https://doi.org/10.1007/s12155-021-10348-3.

44. Phanphanich M, Mani S. Impact of torrefaction on the grindability and fuel characteristics of forest biomass. Bioresour Technol. 2011;102(2):1246–53. https://doi.org/10.1016/j.biortech.2010.08.028.

45. Adeleke AA, Odusote JK, Ikubanni PP, Lasode OA, Malathi M, Paswan D. Essential basics on biomass torrefaction, densification and utilization. Int J Energy Res. 2021;45(2):1375–95. https://doi.org/10.1002/er.5884.

46. Chew JJ, Doshi V. Recent advances in biomass pretreatment: torrefaction fundamentals and technology. Renew Sustain Energy Rev. 2011;15(8):4212–22. https://doi.org/10.1016/j.rser.2011.09.017.

47. Dzurenda L, Banski A. Influence of moisture content of combusted wood on the thermal efficiency of a boiler. Arch Thermodyn. 2017;38(1):63–74. https://doi.org/10.1515/aoter-2017-0004.

48. Loh SK. The potential of the Malaysian oil palm biomass as a renewable energy source. Energy Convers Manag. 2017;141:285–98. https://doi.org/10.1016/j.enconman.2016.08.081.

49. Singh YD, Mahanta P, Bora U. Comprehensive characterization of lignocellulosic biomass through proximate, ultimate and compositional analysis for bioenergy production. Renew Energy. 2017;103:490–500. https://doi.org/10.1016/j.renene.2016.11.039.

50. Bach Q-V, Skreiberg Ø. Upgrading biomass fuels via wet torrefaction: a review and comparison with dry torrefaction. Renew Sustain Energy Rev. 2016;54:665–77. https://doi.org/10.1016/j.rser.2015.10.014.

51. Wu K-T, Tsai C-J, Chen C-S, Chen H-W. The characteristics of torrefied microalgae. Appl Energy. 2012;100:52–7. https://doi.org/10.1016/j.apenergy.2012.03.002.

52. Granados DA, Ruiz RA, Vega LY, Chejne F. Study of reactivity reduction in sugarcane bagasse as consequence of a torrefaction process. Energy. 2017;139:818–27. https://doi.org/10.1016/j.energy.2017.08.013.

53. Ramakrishna V, Singh AK, Bayen GK, Masto RE, Meena RK, Singh PK, et al. Torrefaction of agro-wastes (Palmyra palm shell and Redgram stalk): characterization of the physicochemical properties and mechanical strength of binderless pellets. Biomass Convers Biorefinery. 2021. https://doi.org/10.1007/s13399-021-01720-6.

54. Adeleke AA, Odusote JK, Ikubanni PP, Lasode OA, Malathi M, Paswan D. The ignitability, fuel ratio and ash fusion temperatures of torrefied woody biomass. Heliyon. 2020;6(3):e03582. https://doi.org/10.1016/j.heliyon.2020.e03582.

55. Legemza J, Fröhlichová M, Findorák R. Biomass and carbon fuels in metallurgy. Boca Raton: CRC Press; 2019.

56. Anukam A, Mamphweli S, Reddy P, Meyer E, Okoh O. Pre-processing of sugarcane bagasse for gasification in a downdraft biomass gasifier system: a comprehensive review. Renew Sustain Energy Rev. 2016;66:775–801. https://doi.org/10.1016/j.rser.2016.08.046.

57. Carroll JP, Finnan J. Physical and chemical properties of pellets from energy crops and cereal straws. Biosyst Eng. 2012;112(2):151–9. https://doi.org/10.1016/j.biosystemseng.2012.03.012.

58. Vassilev SV, Vassileva CG, Song Y-C, Li W-Y, Feng J. Ash contents and ash-forming elements of biomass and their significance for solid biofuel combustion. Fuel. 2017;208:377–409. https://doi.org/10.1016/j.fuel.2017.07.036.

59. Niu Y, Lv Y, Lei Y, Liu S, Liang Y, Wang D, et al. Biomass torrefaction: properties, applications, challenges, and economy. Renew Sustain Energy Rev. 2019;115:109395. https://doi.org/10.1016/j.rser.2019.109395.

60. Saidur R, Abdelaziz EA, Demirbas A, Hossain MS, Mekhilef S. A review on biomass as a fuel for boilers. Renew Sustain Energy Rev. 2011;15(5):2262–89. https://doi.org/10.1016/j.rser.2011.02.015.

61. Basu P. Chapter 3: biomass characteristics. In: Basu P, editor. Biomass gasification, pyrolysis and torrefaction. 3rd ed. London: Academic Press; 2018. p. 49–91.

62. van Loo S, Koppejan J. IEA bioenergy, task 32: biomass combustion and co-firing. Handbook of biomass combustion and co-firing. Enschede: Twente University Press; 2002.

63. Strezov V, Evans TJ. Biomass processing technologies. Boca Raton: Taylor and Francis; 2014.

64. Mei Y, Liu R, Yang Q, Yang H, Shao J, Draper C, et al. Torrefaction of cedarwood in a pilot scale rotary kiln and the influence of industrial flue gas. Bioresour Technol. 2015;177:355–60. https://doi.org/10.1016/j.biortech.2014.10.113.

65. Ramos-Carmona S, Martínez JD, Pérez JF. Torrefaction of patula pine under air conditions: a chemical and structural characterization. Ind Crops Prod. 2018;118:302–10. https://doi.org/10.1016/j.indcrop.2018.03.062.

66. Barta-Rajnai E, Wang L, Sebestyén Z, Barta Z, Khalil R, Skreiberg Ø, et al. Comparative study on the thermal behavior of untreated and various torrefied bark, stem wood, and stump of Norway spruce. Appl Energy. 2017;204:1043–54. https://doi.org/10.1016/j.apenergy.2017.05.057.

67. Kethobile E, Ketlogetswe C, Gandure J. Torrefaction of non-oil Jatropha curcas L. (Jatropha) biomass for solid fuel. Heliyon. 2020;6(12):e05657. https://doi.org/10.1016/j.heliyon.2020.e05657.

68. Obernberger I, Brunner T, Bärnthaler G. Chemical properties of solid biofuels—significance and impact. Biomass Bioenergy. 2006;30(11):973–82. https://doi.org/10.1016/j.biombioe.2006.06.011.

69. Oyebode WA, Ogunsuyi HO. Impact of torrefaction process temperature on the energy content and chemical composition of stool tree (Alstonia congenisis Engl.) woody biomass. Curr Res Green Sustain Chem. 2021;4:100115. https://doi.org/10.1016/j.crgsc.2021.100115.

70. Kumar M, Sabbarwal S, Mishra PK, Upadhyay SN. Thermal degradation kinetics of sugarcane leaves (Saccharum officinarum L.) using thermo-gravimetric and differential scanning calorimetric studies. Bioresour Technol. 2019;279:262–70. https://doi.org/10.1016/j.biortech.2019.01.137.

71. Mishra RK, Mohanty K. Pyrolysis kinetics and thermal behavior of waste sawdust biomass using thermogravimetric analysis. Bioresour Technol. 2018;251:63–74. https://doi.org/10.1016/j.biortech.2017.12.029.

72. He Y, Chang C, Li P, Han X, Li H, Fang S, et al. Thermal decomposition and kinetics of coal and fermented cornstalk using thermogravimetric analysis. Bioresour Technol. 2018;259:294–303. https://doi.org/10.1016/j.biortech.2018.03.043.

73. Siddiqi H, Bal M, Kumari U, Meikap BC. In-depth physio-chemical characterization and detailed thermo-kinetic study of biomass wastes to analyze its energy potential. Renew Energy. 2020;148:756–71. https://doi.org/10.1016/j.renene.2019.10.162.

74. Gajera ZR, Verma K, Tekade SP, Sawarkar AN. Kinetics of co-gasification of rice husk biomass and high sulphur petroleum coke with oxygen as gasifying medium via TGA. Bioresour Technol Rep. 2020;11:100479. https://doi.org/10.1016/j.biteb.2020.100479.

75. Özsin G, Pütün AE. TGA/MS/FT-IR study for kinetic evaluation and evolved gas analysis of a biomass/PVC co-pyrolysis process. Energy Convers Manag. 2019;182:143–53. https://doi.org/10.1016/j.enconman.2018.12.060.

76. Islam MdA, Asif M, Hameed BH. Pyrolysis kinetics of raw and hydrothermally carbonized Karanj (Pongamia pinnata) fruit hulls via thermogravimetric analysis. Bioresour Technol. 2015;179:227–33. https://doi.org/10.1016/j.biortech.2014.11.115.

77. Gupta GK, Mondal MK. Kinetics and thermodynamic analysis of maize cob pyrolysis for its bioenergy potential using thermogravimetric analyzer. J Therm Anal Calorim. 2019;137(4):1431–41. https://doi.org/10.1007/s10973-019-08053-7.

78. Chen W-H, Lin B-J, Lin Y-Y, Chu Y-S, Ubando AT, Show PL, et al. Progress in biomass torrefaction: principles, applications and challenges. Prog Energy Combust Sci. 2021;82:100887. https://doi.org/10.1016/j.pecs.2020.100887.